Universities of Leeds, Sheffield and York
http://eprints.whiterose.ac.uk/

Generation of coherent magnetic fields in sheared inhomogeneous turbulence: no need for rotation?

Nicolas Leprovost and Eun-jin Kim[1]

Department of Applied Mathematics, University of Sheffield, Sheffield S3 7RH, UK

(Dated: 10 December 2010)

Coherent magnetic fields are often believed to be generated by the combination of stretching by differential rotation and turbulent amplification of magnetic field, via the so-called α effect. The latter is known to exist in helical turbulence, which is envisioned to arise due to both rotation and convection in solar-type stars. In this contribution, a turbulent flow driven by a nonhelical inhomogeneous forcing, and its kinematic dynamo action are studied for a uniform magnetic field in the background of a linear shear flow. By using a quasi-linear analysis and a non-perturbative method utilizing a time-dependent wave number, turbulence property and electromotive force are computed for an arbitrary shear strength. Due to the large-scale shear flow, the turbulence is highly anisotropic, as a consequence, the electromotive force. The latter is found to exist even without rotation due to the combined effect of shear flow and inhomogeneous forcing, containing not only the α effect but also magnetic pumping (the γ effect representing a transport of magnetic flux by turbulence). Specifically, without shear, only the magnetic pumping exists, aligned with the direction of inhomogeneity. For a weak but non-zero shear, the combined effects of shear and inhomogeneous forcing modify the structure of the magnetic pumping when the inhomogeneity is in the plane of the shear flow, the magnetic pumping becoming bi-dimensional in that plane. It also induces an α tensor which has non-diagonal components. When the inhomogeneity is perpendicular to the plane of the shear flow, the α effect has three non-zero diagonal components and one off-diagonal component. However, for a sufficiently strong shear, the γ and α effects are suppressed due to shear stabilization which damps turbulence. A simplified dynamo model is then proposed where a large-scale dynamo arises due to the combined effect of shear flow and inhomogeneous forcing. In particular, the growth of a large-scale axisymmetric magnetic field is demonstrated in the case of an inhomogeneity which is perpendicular to the plane of the shear flow. Interesting implications of these results for the structure of magnetic fields in star with slow rotation are discussed.

2

I.   INTRODUCTION

Magnetic fields observed in astrophysical and laboratory plasmas are thought to be the result of dynamo action. In mean-field dynamo, the amplification of large-scale magnetic field relies on two processes: the stretching of magnetic field lines by velocity gradients (the Ω effect) and the effect of turbulent cyclonic motion (the α effect). The latter is associated with the helicity of the turbulent flow. For instance, in astrophysical plasmas (e.g. the Sun), helicity is very likely to be present due to a combination of rotation and convection. Recently, the efficiency of the α effect in the limit of large magnetic Reynolds number has been discussed[1] and other means of dynamo action have been sought after. For instance it has been shown that the addition of shear flow in rotating convection could drive a dynamo[2–4]. Furthermore, numerical simulations have shown dynamo action at large scale in *non-helical turbulence* in the presence of shear[5]. This is an interesting result as the α effect is often thought to vanish in a turbulence without helicity. Various mechanisms have been invoked to explain this large-scale dynamo in non-helical turbulence: stochastic α effect[6], shear amplification of small-scale dynamo[7], magnetic effect driven by current helicity flux[8] or negative diffusivity[9].

Mathematically, the mean-field dynamo[10,11] is based on the following averaged induction equation for a large-scale mean magnetic field $\langle \mathbf{B} \rangle$ in a conducting fluid $\mathbf{U}$:

$$\partial_t \langle \mathbf{B} \rangle + \langle \mathbf{U} \rangle \cdot \nabla \langle \mathbf{B} \rangle = \langle \mathbf{B} \rangle \cdot \nabla \langle \mathbf{U} \rangle + \eta \nabla^2 \langle \mathbf{B} \rangle + \nabla \times \mathcal{E} \ . \tag{1}$$

Here η is the ohmic diffusivity; the $\langle \bullet \rangle$ stands for an average on the realization of the small-scale fields. The first term on the RHS of Eq. (1) is the Ω effect, representing the stretching of magnetic field lines by gradient of the mean flow $\nabla \langle \mathbf{U} \rangle$. It is an efficient mechanism to create toroidal field from a poloidal field in a system with differential rotation[10]. The last term $\mathcal{E} = \langle \mathbf{u} \times \mathbf{b} \rangle$ in Eq. (1) is the electromotive force, which is often taken to be linear in the mean magnetic field $\langle \mathbf{B} \rangle$ with the following expansion:

$$\mathcal{E}_i = a_{ij} \langle B_j \rangle + b_{ijk} \frac{\partial \langle B_j \rangle}{\partial x_k} + \dots \ . \tag{2}$$

In the kinematic limit where the magnetic field has no back reaction on the velocity field, the tensors a_{ij} and b_{ijk} depend only on the properties of the velocity field. In this paper, a uniform magnetic field is considered in which case only the first term in Eq. (2) survives.

By decomposing the tensor a_{ij} in its symmetric and antisymmetric part, the electromotive force can then be written as:

$$\mathcal{E}_i = \alpha_{ij}\langle B_j\rangle + (\gamma \times \langle \mathbf{B}\rangle)_i \tag{3}$$

The first term on the right-hand side (proportional to the symmetric part of the a_{ij} tensor: $\alpha_{ij} = (a_{ij} + a_{ji})/2$) is the α effect. It is often believed to be the main source (in combination with the Ω effect noted previously) for generation of large-scale magnetic field in the Sun. Note however that it was shown by previous authors[11,12] that anisotropy or inhomogeneity combined with rotation or large-scale shear flow can give rise to the α effect. The second term on the right-hand side of Eq. (3), proportional to the anti-symmetric part of the a_{ij} tensor, describes the transport of mean magnetic flux by turbulence and is present only in an anisotropic or inhomogeneous turbulence[13].

The purpose of this paper is to investigate the structure of the electromotive force in a forced turbulence driven by a non-helical inhomogeneous forcing in the presence of a large-scale shear flow. In the Sun, the inhomogeneous forcing would physically arise due to rotation and/or convection in the convection zone. While our study is limited to a kinematic dynamo where the nonlinear backreaction of magnetic field onto the flow is neglected, the turbulent flow is obtained dynamically by the forcing, and evolves consistently subject to the given shear flow. That is, the focus of our study is to examine the influences of a shear flow on magnetic field not only directly but also indirectly through its effect on the turbulent flow. To this end, we incorporate the effect of the shear non-perturbatively by using time-dependent wavenumber and compute the electromotive force for arbitrary strength of the shear. Our non-perturbative approach is thus in contrast to previous works[12,14], which are valid only for weak shear. We first show that the combined effect of shear flow and inhomogeneity leads to non-vanishing α and γ effects. However, as the strength of shear increases, we show, for the first time, that these shear-induced α and β effects are severely reduced for sufficiently strong shear. This is due to shear stabilization which damps turbulence: a strong shear flow influences large-scale magnetic field $\langle \mathbf{B}\rangle$ indirectly by reducing turbulent transport[15].

In section II, the model is introduced. Sections III, IV and V present the calculations of the magnetohydrodynamics fluctuations, the statistics of turbulence (intensity and helicity) and the electromotive force, respectively. Section VI presents the results in the case of a weak inhomogeneity. Section VII presents a two-dimensional mean-field model where large-

4

scale dynamo action arises solely due to the combined action of inhomogeneity and shear. Discussion of the results and physical implications are presented in Section VIII.

II.   MODEL

Calculations are performed in the kinematic limit where the back-reaction of the magnetic field on the velocity is neglected. From the physical point of view, this amounts to considering a very weak magnetic field and ignoring the Lorentz force on the fluid which is quadratic in the magnetic field. For an incompressible conducting fluid, the resulting equations of motion are:

$$\partial_t \mathbf{U} + \mathbf{U} \cdot \nabla \mathbf{U} = -\nabla p + \nu \Delta \mathbf{U} + \mathbf{f} \ , \tag{4}$$

$$\partial_t \mathbf{B} + \mathbf{U} \cdot \nabla \mathbf{B} = \mathbf{B} \cdot \nabla \mathbf{U} + \eta \Delta \mathbf{B} \ ,$$

$$\nabla \cdot \mathbf{U} = \nabla \cdot \mathbf{B} = 0 \ .$$

Here $\mathbf{B}$ is the magnetic field given in units of Alfvén speed, p is the pressure, and $\mathbf{f}$ is a small-scale forcing. To study the effect of shear flows and magnetic fields on small-scale turbulence, a large scale flow to be a linear shear flow of $\langle \mathbf{U} \rangle = -x\mathcal{A}\mathbf{e_y}$ with a constant shear $\mathcal{A}$ and a uniform large-scale magnetic field $\langle \mathbf{B} \rangle$ are prescribed. To solve the equations for the fluctuating velocity field, $\mathbf{u} = \mathbf{U} - \langle \mathbf{U} \rangle$, and magnetic field, $\mathbf{b} = \mathbf{B} - \langle \mathbf{B} \rangle$, the quasi-linear approximation is used: the interaction between fluctuating fields is negligible compared to the interaction between large and small-scale fields. The equations for the fluctuating fields can then be written as:

$$\partial_t \mathbf{u} + \langle \mathbf{U} \rangle \cdot \nabla \mathbf{u} + \mathbf{u} \cdot \nabla \langle \mathbf{U} \rangle = -\nabla p + \nu \Delta \mathbf{u} + \mathbf{f} \ , \tag{5}$$

$$\partial_t \mathbf{b} + \mathbf{u} \cdot \nabla \langle \mathbf{B} \rangle + \langle \mathbf{U} \rangle \cdot \nabla \mathbf{b} = \mathbf{b} \cdot \nabla \langle \mathbf{U} \rangle + \langle \mathbf{B} \rangle \cdot \nabla \mathbf{u} + \eta \Delta \mathbf{b} \ ,$$

$$\nabla \cdot \mathbf{u} = \nabla \cdot \mathbf{b} = 0 \ .$$

Here, we have ignored nonlinear term $(\mathbf{u}{\cdot}\nabla\mathbf{u})$ in comparison with the advection by the large-scale flow $(\langle \mathbf{U} \rangle{\cdot}\nabla\mathbf{u})$ and the stretching $(\mathbf{u}{\cdot}\nabla\langle \mathbf{U} \rangle)$. Note that this quasi-linear approximation, strictly valid for a small Rossby number $u/\mathcal{A}l \ll 1$, has been shown to work well in a strongly sheared turbulence as turbulence becomes weak by shear stabilization (e.g. see[16],[17], and references therein). Here, u is the magnitude of the turbulent intensity and l is the turbulence scale.

In this paper, we compute the turbulence intensity (given by $\langle u^2 \rangle$), the turbulence helicity (given by $\langle \mathbf{u} \cdot \nabla \mathbf{u} \rangle$) and the electromotive force (given by $\langle \mathbf{u} \times \mathbf{b} \rangle$). To compute these quantities, the two-point correlation of the forcing needs to be prescribed. Here, a short correlated (with correlation time τ_f) forcing is considered. Specifically, in Fourier space, the correlation function of the forcing is taken as:

$$\langle \tilde{f}_i(\mathbf{k_1}, t_1) \tilde{f}_j(\mathbf{k_2}, t_2) \rangle = \tau_f (2\pi)^3 \delta(t_1 - t_2) \phi_{ij}(\mathbf{k_1}, \mathbf{k_2}) , \tag{6}$$

where ϕ_{ij} is the power spectrum. The inhomogeneous turbulence model of Kichatinov[18] is used. In this model, the power spectrum function is given by:

$$\phi_{ij}(\mathbf{k_1}, \mathbf{k_2}) = \frac{E(k, \mathbf{s})}{8\pi k^4} \left[k^2 \delta_{ij} - \left(1 + \frac{s^2}{4k^2} \right) k_i k_j + \frac{s_i k_j - s_j k_i}{2} + \frac{s_i s_j}{4} \right] . \tag{7}$$

where $\mathbf{k} = (\mathbf{k}_1 - \mathbf{k}_2)/2$ and $\mathbf{s} = \mathbf{k}_1 + \mathbf{k}_2$. Note that the homogeneous isotropic forcing is recovered by setting $E(k, \mathbf{s}) = E(k)\delta(\mathbf{s})$. $E(k, \mathbf{s})$ in Eq. (7) is related to the correlation functions of the forcing as:

$$\langle \mathbf{f}(t_1, \mathbf{x}) \cdot \mathbf{f}(t_2, \mathbf{x}) \rangle = \delta(t_1 - t_2) \frac{\tau_f}{(2\pi)^3} \int d^3 s \int_0^{+\infty} dk \, \cos\left[\mathbf{s} \cdot \mathbf{x} \right] E(k, \mathbf{s}) , \tag{8}$$

$$\nabla \langle \mathbf{f}(t_1, \mathbf{x}) \cdot \mathbf{f}(t_2, \mathbf{x}) \rangle = -\delta(t_1 - t_2) \frac{\tau_f}{(2\pi)^3} \int d^3 s \int_0^{+\infty} dk \, \mathbf{s} \, \sin\left[\mathbf{s} \cdot \mathbf{x} \right] E(k, \mathbf{s}) .$$

It is clearly seen that the gradient of the forcing is the source of inhomogeneity. Note that the positivity of the forcing intensity at any spatial point x implies the following inequality:

$$E_0(k, \mathbf{x}) \equiv \int d^3 s \cos\left[\mathbf{s} \cdot \mathbf{x} \right] E(k, \mathbf{s}) \geq 0 , \tag{9}$$

for all values of k and $\mathbf{x}$ (as $E_0(k,\mathbf{x})$ is the energy density in k-space). Similarly, the k-space density of the gradient of forcing intensity is defined as:

$$\mathbf{G_0}(k, \mathbf{x}) \equiv \int d^3 s \, \mathbf{s} \sin\left[\mathbf{s} \cdot \mathbf{x} \right] E(k, \mathbf{s}) . \tag{10}$$

Note that unlike $E_0(k, \mathbf{x})$, the components of this vector $\mathbf{G}_0$ do not need to be positive.

In the following three sections, the details of our calculations are presented in three steps:

1. Computation of the fluctuating velocity and magnetic field $\mathbf{u}(\mathbf{x}, t)$ and $\mathbf{b}(\mathbf{x}, t)$ in Sec. III

2. Computation of the turbulence intensity and helicity in Sec. IV

3. Computation of the electromotive force in Sec. V

As the next three sections involve technical details of calculations, the reader who is only interested in main results may wish to go directly to Section VI where the calculations are completed in the limit of weak inhomogeneity and the results are presented.

III. MAGNETOHYDRODYNAMICS FLUCTUATIONS

In this paper, an unit magnetic Prandtl number ($\nu = \eta$) and, following the seminal work of Lord Kelvin[19], a time-dependent Fourier transform[20] is used to non-perturbatively incorporate the effect of shearing by large-scale shear flow:

$$Y(\mathbf{x}, t) = \frac{1}{(2\pi)^3} \int d\mathbf{k} \ e^{i\left[k_x(t)x + k_y y + k_z z\right]} \tilde{Y}(\mathbf{k}, t) \ . \tag{11}$$

Transforming the time variable t to $\tau = k_x(t)/k_y = k_x(t_0)/k_y + \mathcal{A}(t - t_0)$ and using the new variables $\hat{\mathbf{u}} = \tilde{\mathbf{u}} \exp[\nu(k_H^2 t + k_x^3/3k_y\mathcal{A})]$ (and similarly for $\hat{\mathbf{b}}$, $\hat{\mathbf{f}}$ and $\hat{p}$) where $k_H^2 = k_y^2 + k_z^2$ to absorb the diffusive term, Eq. (5) can be written:

$$\partial_\tau \hat{u}_i = \hat{u}_x \delta_{i2} - ik_y \theta_i \hat{p}/\mathcal{A} + \hat{f}_i/\mathcal{A} \ , \tag{12}$$

$$\partial_\tau \hat{b}_i = -\hat{b}_x \delta_{i2} + \frac{ik_y}{\mathcal{A}}(\langle \mathbf{B} \rangle \cdot \theta)\hat{u}_i \ ,$$

$$\tau \hat{u}_x + \hat{u}_y + \beta \hat{u}_z = \tau \hat{b}_x + \hat{b}_y + \beta \hat{b}_z = 0 \ .$$

Here, $\beta = k_z/k_y$; $\theta_i = (\tau, 1, \beta)$. Note that since the first equation of (12) does not involve the magnetic field, the solution to $\hat{u}_i$ is the same as in the hydrodynamical case (see Eq. (7) of Kim[20]):

$$\hat{u}_x(\mathbf{k}, \tau) = \int_a^\tau \hat{h}_1(t) J_x(t, \tau) \, dt \ , \tag{13}$$

$$\hat{u}_y(\mathbf{k}, \tau) = \int_a^\tau \left[-\hat{h}_1(t) J_{y1}(t, \tau) - \hat{h}_2(t) J_{y2}(t, \tau)\right] dt \ ,$$

$$\hat{u}_z(\mathbf{k}, \tau) = \int_a^\tau \left[-\hat{h}_1(t) J_{z1}(t, \tau) + \hat{h}_2(t) J_{z2}(t, \tau)\right] dt \ .$$

Here, $\kappa = 1 + \beta^2$; $a = k_x(t_0)/k_y$ is the initial value of the x-component of the wave vector (non-dimensionalized by the y-component); the following functions are defined :

$$\hat{h}_1(t) = \left[\kappa \hat{f}_x(t) - a\hat{f}_y(t) - a\beta \hat{f}_z(t)\right]/\mathcal{A} \ , \tag{14}$$

7

$$\hat{h}_2(t) = \left[-\beta \hat{f}_y(t) + \hat{f}_z(t)\right]/\mathcal{A} \,,$$

$$T(x) = \frac{1}{\sqrt{\kappa}} \arctan\left(\frac{x}{\sqrt{\kappa}}\right) \,,$$

$$J_x(t,\tau) = \frac{1}{\kappa + \tau^2} \,,$$

$$J_{y1}(t,\tau) = \frac{1}{\kappa}\left\{\frac{\tau}{\kappa + \tau^2} - \beta^2 \left[T(\tau) - T(t)\right]\right\} \,,$$

$$J_{y2}(t,\tau) = \frac{\beta}{\kappa} \,,$$

$$J_{z1}(t,\tau) = \frac{\beta}{\kappa}\left\{\frac{\tau}{\kappa + \tau^2} + T(\tau) - T(t)\right\} \,,$$

$$J_{z2}(t,\tau) = \frac{1}{\kappa} \,.$$

For the calculation of the fluctuating magnetic field, the following two cases are considered:

1. for $\mathbf{B_0} = B_0 \mathbf{e_x}$ where $\mathbf{B_0}$ is parallel to the gradient of the shear flow. Note that in this case, the term $(\langle \mathbf{B} \rangle \cdot \theta)$ in the second equation of (12) is proportional to τ

2. for $\mathbf{B_0} = B_0 \mathbf{e_y}$ and $\mathbf{B_0} = B_0 \mathbf{e_z}$ where $\mathbf{B_0}$ is perpendicular to the gradient of the shear flow where $(\langle \mathbf{B} \rangle \cdot \theta)$ in Eq. (12) is independent of τ.

1. *Magnetic field in the x direction*

In the case where the large-scale magnetic field is in the direction of the shear ($\langle \mathbf{B} \rangle = B_0 \mathbf{e_x}$), the second equation of (12) can be rewritten:

$$\partial_\tau \hat{b}_i = -\hat{b}_x \delta_{i2} + \frac{ik_y B_0}{\mathcal{A}} \tau \hat{u}_i \,. \tag{15}$$

Using the expression (13) for the fluctuating velocity, the magnetic fluctuations can be obtained from Eq. (12) by integration as:

$$\hat{b}_x = \frac{ik_y B_0}{\mathcal{A}} \int_a^\tau dt \hat{h}_1(t) K_x(t,\tau) \, dt \,, \tag{16}$$

$$\hat{b}_y = \frac{ik_y B_0}{\mathcal{A}} \int_a^\tau dt \left[-\hat{h}_1(t) K_{y1}(t,\tau) - \hat{h}_2(t) K_{y2}(t,\tau)\right] \,,$$

$$\hat{b}_z = \frac{ik_y B_0}{\mathcal{A}} \int_a^\tau dt \left[-\hat{h}_1(t) K_{z1}(t,\tau) + \hat{h}_2(t) K_{z2}(t,\tau)\right] \,.$$

Here, the following functions are defined as:

$$J_1(t,\tau) = (\tau^2 - \kappa)\left\{T(\tau) - T(t)\right\} + (\tau - t) \,, \tag{17}$$

8

$$K_x(t,\tau) = \frac{1}{2}\log\left[\frac{\kappa + \tau^2}{\kappa + t^2}\right] \ ,$$

$$K_{y1}(t,\tau) = \frac{1}{2\kappa}\left\{-\beta^2 J_1(t,\tau) + \kappa\tau\log\left[\frac{\kappa + \tau^2}{\kappa + t^2}\right]\right\} \ ,$$

$$K_{y2}(t,\tau) = \frac{\beta}{2\kappa}\left(\tau^2 - t^2\right) \ ,$$

$$K_{z1}(t,\tau) = \frac{\beta}{2\kappa}J_1(t,\tau) \ ,$$

$$K_{z2}(t,\tau) = \frac{1}{2\kappa}\left(\tau^2 - t^2\right) \ .$$

2. Magnetic field in the y or z direction

In the case where the large-scale magnetic field is in the y-direction ($\langle \mathbf{B}\rangle = B_0\mathbf{e_y}$), the second equation of (12) can be rewritten:

$$\partial_\tau \hat{b}_i = -\hat{b}_x\delta_{i2} + \frac{ik_yB_0}{\mathcal{A}}\hat{u}_i \ . \tag{18}$$

Using expression (13) for the fluctuating velocity, the magnetic fluctuations can be obtained from Eq. (12) by integration as:

$$\hat{b}_x = \frac{ik_yB_0}{\mathcal{A}}\int_a^\tau dt\hat{h}_1(t)L_x(t,\tau)\,dt \ , \tag{19}$$

$$\hat{b}_y = \frac{ik_yB_0}{\mathcal{A}}\int_a^\tau dt\left[-\hat{h}_1(t)L_{y1}(t,\tau) - \hat{h}_2(t)L_{y2}(t,\tau)\right] \ ,$$

$$\hat{b}_z = \frac{ik_yB_0}{\mathcal{A}}\int_a^\tau dt\left[-\hat{h}_1(t)L_{z1}(t,\tau) + \hat{h}_2(t)L_{z2}(t,\tau)\right] \ .$$

Here,

$$J_2(t,\tau) = \tau\left\{T(\tau) - T(t)\right\} \ , \tag{20}$$

$$L_x(t,\tau) = T(\tau) - T(t) \ ,$$

$$L_{y1}(t,\tau) = \frac{J_2(t,\tau)}{\kappa} \ ,$$

$$L_{y2}(t,\tau) = \frac{\beta}{\kappa}\left(\tau - t\right) \ ,$$

$$L_{z1}(t,\tau) = \frac{\beta}{\kappa}J_2(t,\tau) \ ,$$

$$L_{z2}(t,\tau) = \frac{1}{\kappa}\left(\tau - t\right) \ .$$

Finally, the results in the case where a large-scale magnetic field is in the z-direction ($\langle \mathbf{B}\rangle = B_0\mathbf{e_z}$) can be obtained by replacing k_yB_0 by k_zB_0 in Eq. (18) and in front of the integrals in Eq. (19).

9

IV. TURBULENCE STATISTICS TRIGGERED BY AN INHOMOGENEOUS FORCING

We start with the calculation of the turbulence intensity in the x direction, which can be written as:

$$\langle u_x^2 \rangle = \frac{1}{(2\pi)^6 \mathcal{A}} \int d\mathbf{k_1} \int d\mathbf{k_2} \, e^{i(\mathbf{k_1}+\mathbf{k_2})\cdot\mathbf{x}} \phi_{11}(\mathbf{k_1}, \mathbf{k_2}) \int_a^\infty e^{-2\xi\{Q(\tau)-Q(a)\}} J_x(\mathbf{k_1}) J_x(\mathbf{k_2}) d\tau \qquad (21)$$

$$= \frac{1}{(2\pi)^6 \mathcal{A}} \int d\mathbf{s} \int d\mathbf{k} \, e^{i\mathbf{s}\cdot\mathbf{x}} \phi_{11}(\mathbf{k}+\mathbf{s}/2, \mathbf{k}-\mathbf{s}/2) \int_a^\infty e^{-2\xi\{Q(\tau)-Q(a)\}} J_x(\mathbf{k}+\mathbf{s}/2) J_x(\mathbf{k}-\mathbf{s}/2) d\tau$$

Here: $\xi = \nu k_y^2/\mathcal{A}$ and $Q(x) = \kappa x + x^3/3 + \mathcal{G}^2 x$; the functions J_x is defined in Eq. (14). To find the overall behavior of the turbulence intensity, one needs to take into account all the wave-numbers and perform the k-integration. To this end, we write the wave-vector in spherical coordinates ($k_x = k\cos\theta$, $k_y = k\sin\theta\cos\phi$ and $k_z = k\sin\theta\sin\phi$) and perform the average over θ and ϕ. By setting $\phi_{11} \equiv f_{11}E(k,\mathbf{s})/(8\pi k^2)$ and performing the angular integration, Eq. (21) can be rewritten as:

$$\langle u_x^2 \rangle = \frac{\tau_f}{(2\pi)^2} \int d\mathbf{s} \int dk \, \cos[\mathbf{s}\cdot\mathbf{x}] \frac{E(k,s_x)}{8\pi\nu k^2} I_x^*(\xi_*, \mathbf{s}) \qquad (22)$$

where:

$$I_x^*(\xi_*, \mathbf{s}) = \frac{1}{2\pi} \int_{-\pi}^{+\pi} d\phi \int_0^\pi d\theta \frac{1}{\sin\theta\cos^2\phi} \xi \int_a^\infty e^{-2\xi\{Q(\tau)-Q(a)\}} f_{11} J_x^+ J_x^- d\tau \qquad (23)$$

Here, $\xi_* = \nu k^2/\mathcal{A}$ and the superscript $+$ means that the argument is $\mathbf{k}+\mathbf{s}/2$ whereas the superscript $-$ means that the argument is $\mathbf{k}-\mathbf{s}/2$. Similarly, the turbulence intensity in the other two directions can be obtained as:

$$\langle u_y^2 \rangle = \frac{\tau_f}{(2\pi)^2} \int d\mathbf{s} \int dk \, \cos[\mathbf{s}\cdot\mathbf{x}] \frac{E(k,s_x)}{8\pi\nu k^2} I_y^*(\xi_*, \mathbf{s}) \,, \qquad (24)$$

$$\langle u_z^2 \rangle = \frac{\tau_f}{(2\pi)^2} \int d\mathbf{s} \int dk \, \cos[\mathbf{s}\cdot\mathbf{x}] \frac{E(k,s_x)}{8\pi\nu k^2} I_z^*(\xi_*, \mathbf{s}) \,,$$

where the following integrals have been defined:

$$I_y^*(\xi_*, \mathbf{s}) = \frac{1}{2\pi} \int_{-\pi}^{+\pi} d\phi \int_0^\pi d\theta \frac{1}{\sin\theta\cos^2\phi} \xi \int_a^\infty d\tau e^{-2\xi\{Q(\tau)-Q(a)\}} \times \qquad (25)$$
$$\left[f_{11} J_{y1}^+ J_{y1}^- + f_{22} J_{y2}^+ J_{y2}^- + f_{12} J_{y1}^+ J_{y2}^- + f_{21} J_{y1}^- J_{y2}^+ \right] \,,$$

$$I_z^*(\xi_*, \mathbf{s}) = \frac{1}{2\pi} \int_{-\pi}^{+\pi} d\phi \int_0^\pi d\theta \frac{1}{\sin\theta\cos^2\phi} \xi \int_a^\infty d\tau e^{-2\xi\{Q(\tau)-Q(a)\}} \times$$
$$\left[f_{11} J_{z1}^+ J_{z1}^- + f_{22} J_{z2}^+ J_{z2}^- + f_{12} J_{z1}^+ J_{z2}^- + f_{21} J_{z1}^- J_{z2}^+ \right] \,.$$

Here the following definitions have been used: $\phi_{12} \equiv f_{12} E(k, \mathbf{s})/(8\pi k^2)$, $\phi_{21} \equiv f_{21} E(k, \mathbf{s})/(8\pi k^2)$ and $\phi_{22} \equiv f_{22} E(k, \mathbf{s})/(8\pi k^2)$. Note that only the terms in even power of $\mathbf{s}$ have to be kept as the terms in odd power in $\mathbf{s}$ would vanish after angular integration over θ and ϕ in Eqs (22-24).

Note that two cases must be considered separately, the inhomogeneity being in the plane of the shear or perpendicular to it. Indeed, the values of f_{11}, f_{12}, f_{21} and f_{22} are different in these two cases. First, in the case where the inhomogeneity is in the x direction, setting $E(k, \mathbf{s}) = E(k, s_x)\delta(s_y)\delta(s_z)$ in Eq. (7) leads to:

$$f_{11} = \kappa(\kappa + a^2) + \mathcal{G}_*^2 \kappa(3\kappa - a^2) + \mathcal{G}_*^4 \kappa^2 , \tag{26}$$

$$f_{22} = \kappa ,$$

$$f_{12} = f_{21} = 0 ,$$

where $\mathcal{G}_* = s_x/(2k)$. Secondly, when the inhomogeneity is in the z direction, using $E(k, \mathbf{s}) = E(k, s_z)\delta(s_x)\delta(s_y)$ in Eq. (7) gives four relevant components of the power spectrum forcing correlations as:

$$f_{11} = \kappa(\kappa + a^2) - \mathcal{G}_*^2 \kappa(a^4 - \kappa a^2 + 2\kappa^2 - 4\kappa) - \mathcal{G}_*^4(3a^4 + \kappa a^2 + a^2 - \kappa^2) - \mathcal{G}_*^6 a^2(\kappa + a^2) \tag{27}$$

$$f_{22} = \kappa + \mathcal{G}_*^2(3 - a^2 - \beta^2) + \mathcal{G}_*^4 ,$$

$$f_{12} = -a\left[2\sqrt{\kappa + a^2}\mathcal{G}_* + 4\beta\mathcal{G}_*^2 + 4\sqrt{\kappa + a^2}\mathcal{G}_*^3 + \beta\mathcal{G}_*^4 + \sqrt{\kappa + a^2}\mathcal{G}_*^5\right] ,$$

$$f_{21} = -a\left[-2\sqrt{\kappa + a^2}\mathcal{G}_* + 4\beta\mathcal{G}_*^2 - 4\sqrt{\kappa + a^2}\mathcal{G}_*^3 + \beta\mathcal{G}_*^4 - \sqrt{\kappa + a^2}\mathcal{G}_*^5\right] .$$

Here $\mathcal{G}_* = s_z/(2k)$.

Next, the helicity of the flow can be shown as

$$\langle \mathbf{u} \cdot \nabla \times \mathbf{u} \rangle = -\frac{\tau_f}{(2\pi)^2} \int d\mathbf{s} \int dk \ \sin\left[\mathbf{s} \cdot \mathbf{x}\right] \frac{E(k, \mathbf{s})}{8\pi\nu k} H^*(\xi_*, \mathbf{s}) , \tag{28}$$

where:

$$H^*(\xi_*, \mathbf{s}) = \frac{1}{2\pi} \int_{-\pi}^{+\pi} d\phi \int_0^{\pi} d\theta \frac{1}{\cos\phi} \xi \int_a^{\infty} d\tau e^{-2\xi\{Q(\tau)-Q(a)\}} \times \left\{ \right. \tag{29}$$
$$f_{11}\left[a(J_{z1}^+ J_{y1}^- - J_{z1}^- J_{y1}^+) - J_x^+ J_{z1}^- + J_x^- J_{z1}^+ + \beta(-J_x^- J_{y1}^+ + J_x^+ J_{y1}^-)\right]$$
$$+f_{22}a(J_{y2}^+ J_{z2}^- - J_{y2}^- J_{z2}^+)$$
$$+f_{12}\left[a(J_{z1}^+ J_{y2}^- + J_{z2}^- J_{y1}^+) + J_x^+ J_{z2}^- + \beta J_x^+ J_{y2}^-\right]$$
$$+f_{21}\left[-a(J_{z2}^+ J_{y1}^- + J_{z1}^- J_{y2}^+) + J_{z2}^+ J_x^- - \beta J_x^- J_{y2}^+\right] \left. \right\}$$

11

Note that only the terms in odd power of **s** have to be kept as the terms in even power would vanish after integration in Eqs (28). It can be shown that the flow does not possess helicity when the inhomogeneity is in the x-direction: $H^* = 0$ for all values of ξ_* and **s**. On the contrary, when the inhomogeneity is in the z-direction, the helicity does not vanish.

Note that Eqs (22), (24) and (28) involve an integration with respect to **s**. It is thus not straightforward to relate I_x^*, I_y^*, I_z^* and H^* to the energy density (9) and the density of the gradient forcing (10). The **s**-integral cannot be performed in the general case as the prescription of the dependence of the densities on the **s** variable is necessary. The calculation will be carried out in the case of a weak inhomogeneity in Section VI.

V.   ELECTROMOTIVE FORCE

The three components of the electromotive force can be written as:

$$
\mathcal{E} = \begin{pmatrix} \langle u_y b_z - u_z b_y \rangle \\ \langle u_z b_x - u_x b_z \rangle \\ \langle u_x b_y - u_y b_x \rangle \end{pmatrix}
\tag{30}
$$

$$
= \frac{1}{(2\pi)^6} \int d\mathbf{k_1} \int d\mathbf{k_2} e^{i(\mathbf{k_1}+\mathbf{k_2})\cdot\mathbf{x}} \begin{pmatrix} \langle \tilde{u}_y(\mathbf{k_1})\tilde{b}_z(\mathbf{k_2}) - \tilde{u}_z(\mathbf{k_2})\tilde{b}_y(\mathbf{k_1}) \rangle \\ \langle \tilde{u}_z(\mathbf{k_1})\tilde{b}_x(\mathbf{k_2}) - \tilde{u}_x(\mathbf{k_2})\tilde{b}_z(\mathbf{k_1}) \rangle \\ \langle \tilde{u}_x(\mathbf{k_1})\tilde{b}_y(\mathbf{k_2}) - \tilde{u}_y(\mathbf{k_2})\tilde{b}_x(\mathbf{k_1}) \rangle \end{pmatrix} .
$$

To compute the electromotive force, the two cases identified in Sec. III 1 and III 2 are considered separately.

In the case of a large-scale magnetic field in the x-direction, the electromotive force is computed from $\mathcal{E} = \langle \mathbf{u} \times \mathbf{b} \rangle$. Using Eqs. (13) and (16), we obtain

$$
\mathcal{E}_i = \frac{\tau_f}{(2\pi)^3 \mathcal{A}^2} \int d\mathbf{k} \int d\mathbf{s}\, e^{i\mathbf{s}\cdot\mathbf{x}} (iB_0 k_y) \int_a^{+\infty} d\tau e^{-2\xi\{Q(\tau)-Q(a)\}} \times \Big[
\tag{31}
$$

$$
\phi_{11}(\mathbf{k_1},\mathbf{k_2}) \begin{pmatrix} J_{y1}^- K_{z1}^+ - J_{z1}^- K_{y1}^+ \\ J_x^- K_{z1}^+ - J_{z1}^- K_x^+ \\ J_{y1}^- K_x^+ - J_x^- K_{y1}^+ \end{pmatrix} + \phi_{22}(\mathbf{k_1},\mathbf{k_2}) \begin{pmatrix} J_{z2}^- K_{y2}^+ - J_{y2}^- K_{z2}^+ \\ 0 \\ 0 \end{pmatrix}
$$

$$
+\phi_{12}(\mathbf{k_1},\mathbf{k_2}) \begin{pmatrix} J_{y2}^- K_{z1}^+ + J_{z2}^- K_{y1}^+ \\ J_{z2}^- K_x^+ \\ J_{y2}^- K_x^+ \end{pmatrix} - \phi_{21}(\mathbf{k_1},\mathbf{k_2}) \begin{pmatrix} J_{y1}^- K_{z2}^+ + J_{z1}^- K_{y2}^+ \\ J_x^- K_{z2}^+ \\ J_x^- K_{y2}^+ \end{pmatrix} . \Big]
\tag{32}
$$

Here, the J_i's and K_i's functions are defined in Eq. (14) and Eq. (17), respectively; the superscript $+$ means that the argument is $\mathbf{k} + \mathbf{s}/2$ whereas the superscript $-$ means that the argument is $\mathbf{k} - \mathbf{s}/2$.

On the other hand, when $\langle \mathbf{B} \rangle = B_0 e_y$, by using Eqs. (13) and (19), the electromotive force is obtained as:

$$\mathcal{E}_i = \frac{\tau_f}{(2\pi)^3 \mathcal{A}^2} \int d\mathbf{k} \int d\mathbf{s}\, e^{i\mathbf{s} \cdot \mathbf{x}} \left(i B_0 k_y \right) \int_a^{+\infty} d\tau e^{-2\xi\{Q(\tau)-Q(a)\}} \times \Bigg[\tag{33}$$

$$\phi_{11}(\mathbf{k_1}, \mathbf{k_2}) \begin{pmatrix} J_{y1}^- L_{z1}^+ - J_{z1}^- L_{y1}^+ \\ J_x^- L_{z1}^+ - J_{z1}^- L_x^+ \\ J_{y1}^- L_x^+ - J_x^- L_{y1}^+ \end{pmatrix} + \phi_{22}(\mathbf{k_1}, \mathbf{k_2}) \begin{pmatrix} J_{z2}^- L_{y2}^+ - J_{y2}^- L_{z2}^+ \\ 0 \\ 0 \end{pmatrix}$$

$$+\phi_{12}(\mathbf{k_1}, \mathbf{k_2}) \begin{pmatrix} J_{y2}^- L_{z1}^+ + J_{z2}^- L_{y1}^+ \\ J_{z2}^- L_x^+ \\ J_{y2}^- L_x^+ \end{pmatrix} - \phi_{21}(\mathbf{k_1}, \mathbf{k_2}) \begin{pmatrix} J_{y1}^- L_{z2}^+ + J_{z1}^- L_{y2}^+ \\ J_x^- L_{z2}^+ \\ J_x^- L_{y2}^+ \end{pmatrix} \Bigg] .$$

Here, the J_i's and K_i's functions are defined in Eq. (14) and Eq. (20), respectively; the superscript $+$ means that the argument is $\mathbf{k} + \mathbf{s}/2$ whereas the superscript $-$ means that the argument is $\mathbf{k} - \mathbf{s}/2$. In the case where a large-scale magnetic field is in the z-direction ($\langle \mathbf{B} \rangle = B_0 \mathbf{e_z}$), the electromotive force is easily obtained by replacing $B_0 k_y$ with $B_0 k_z$ on the first line of the Eq. (33).

A.   Inhomogeneity in the x direction

By substituting Eq. (26) in Eq. (33), the tensor a_{ij} can be computed in the following form:

$$a_{ij} = \frac{\tau_f}{(2\pi)^3 \mathcal{A}^2} \int d\mathbf{k} \int d s_x\, e^{i s_x x} \left(i k_y \right) \frac{E(k, s_x)}{8\pi k^2} \begin{pmatrix} 0 & 0 & X_3(\mathbf{k}, s_x) \\ 0 & 0 & X_4(\mathbf{k}, s_x) \\ X_1(\mathbf{k}, s_x) & X_2(\mathbf{k}, s_x) & 0 \end{pmatrix}_{ij} \tag{34}$$

Components that are odd functions of β and thus vanish upon $\mathbf{k}$-angular integration were not included in Eq. (34). In Eq. (34), the following integrals are defined :

$$X_1(\mathbf{k}, s_x) = \int_a^{+\infty} d\tau e^{-2\xi\{Q(\tau)-Q(a)\}} f_{11} \left(J_{y1}^- K_x^+ - J_x^- K_{y1}^+ \right) , \tag{35}$$

$$X_2(\mathbf{k}, s_x) = \int_a^{+\infty} d\tau e^{-2\xi\{Q(\tau)-Q(a)\}} f_{11} \left(J_{y1}^- L_x^+ - J_x^- L_{y1}^+ \right) ,$$

13

$$X_3(\mathbf{k}, s_x) = \beta \int_a^{+\infty} d\tau e^{-2\xi\{Q(\tau)-Q(a)\}} \left[f_{11} \left(J_{y1}^- L_{z1}^+ - J_{z1}^- L_x^+ \right) + f_{22} \left(J_{z2}^- L_{y2}^+ - J_{y2}^- L_{z2}^+ \right) \right] ,$$

$$X_4(\mathbf{k}, s_x) = \beta \int_a^{+\infty} d\tau e^{-2\xi\{Q(\tau)-Q(a)\}} f_{11} \left(J_x^- L_{z1}^+ - J_{z1}^- L_{y1}^+ \right) .$$

Here, $\xi = \nu k_y^2/\mathcal{A}$ and $Q(x) = \kappa x + x^3/3 + \mathcal{G}^2 x$, with $\mathcal{G} = s_x/(2k_y)$.

From the tensor a_{ij} in Eq. (34), the turbulent transport of magnetic flux $\gamma_i = -\epsilon_{ijk} a_{jk}/2$ is obtained from its antisymmetric part and the α effect from its symmetric part $\alpha_{ij} = (a_{ij} + a_{ji})/2$. First, the magnetic pumping can be shown to be

$$\gamma = \frac{\tau_f}{(2\pi)^3} \int d\mathbf{k} \int ds_x\, e^{is_x x} \frac{E(k, s_x)}{16\pi\nu^2 k_y^4 k^2} (ik_y)\, \xi^2 \begin{pmatrix} X_2(\mathbf{k}, s_x) - X_4(\mathbf{k}, s_x) \\ X_3(\mathbf{k}, s_x) - X_1(\mathbf{k}, s_x) \\ 0 \end{pmatrix} , \quad (36)$$

Secondly, the symmetric part of the tensor a_{ij} is the α tensor:

$$\alpha_{ij} = \frac{\tau_f}{(2\pi)^3} \int d\mathbf{k} \int ds_x\, e^{is_x x} \frac{E(k, s_x)}{16\pi\nu^2 k_y^4 k^2} (ik_y)\, \xi^2 \times \qquad\qquad (37)$$

$$\begin{pmatrix} 0 & 0 & X_1(\mathbf{k}, s_x) + X_3(\mathbf{k}, s_x) \\ 0 & 0 & X_2(\mathbf{k}, s_x) + X_4(\mathbf{k}, s_x) \\ X_1(\mathbf{k}, s_x) + X_3(\mathbf{k}, s_x) & X_2(\mathbf{k}, s_x) + X_4(\mathbf{k}, s_x) & 0 \end{pmatrix}_{ij} .$$

To find the overall behavior of the γ and α effect, one needs to take into account all the wave-numbers and perform the k-integration. To this end, we write the wave-vector in spherical coordinates ($k_x = k\cos\theta$, $k_y = k\sin\theta\cos\phi$ and $k_z = k\sin\theta\sin\phi$) and perform the integration over θ and ϕ. Eqs. (36) and (37) can then be reduced to

$$\gamma = -\frac{\tau_f}{(2\pi)^2} \int_0^{+\infty} dk \int_{-\infty}^{+\infty} ds_x\, \sin[s_x x] \frac{E(k, s_x)}{8\pi\nu^2 k^3} \begin{pmatrix} \gamma_x^*(\xi_*, \mathcal{G}_*) \\ \gamma_y^*(\xi_*, \mathcal{G}_*) \\ 0 \end{pmatrix} , \quad (38)$$

and

$$\alpha_{ij} = -\frac{\tau_f}{(2\pi)^2} \int_0^{+\infty} dk \int_{-\infty}^{+\infty} ds_x\, \sin[s_x x] \frac{E(k, s_x)}{8\pi\nu^2 k^3} \begin{pmatrix} 0 & 0 & \alpha_{xz}^*(\xi_*, \mathcal{G}_*) \\ 0 & 0 & \alpha_{yz}^*(\xi_*, \mathcal{G}_*) \\ \alpha_{xz}^*(\xi_*, \mathcal{G}_*) & \alpha_{yz}^*(\xi_*, \mathcal{G}_*) & 0 \end{pmatrix}_{ij} (39.)$$

The coefficients in Eqs (38-39) are functions only of $\xi_* = \nu k^2/\mathcal{A}$ and $\mathcal{G}_* = s_x/(2k)$:

$$\gamma_x^*(\xi_*, \mathcal{G}_*) = \frac{1}{2\pi} \int_{-\pi}^{+\pi} d\phi \int_0^\pi d\theta \frac{1}{\sin^3\theta\cos^4\phi} \xi^2 \left[X_2(\mathbf{k}, s_x) - X_4(\mathbf{k}, s_x) \right] , \quad (40)$$

14

$$\gamma_y^*(\xi_*, \mathcal{G}_*) = \frac{1}{2\pi} \int_{-\pi}^{+\pi} d\phi \int_0^{\pi} d\theta \frac{1}{\sin^3\theta \cos^4\phi} \xi^2 \left[X_3(\mathbf{k}, s_x) - X_1(\mathbf{k}, s_x) \right] ,$$

$$\alpha_{xz}^*(\xi_*, \mathcal{G}_*) = \frac{1}{2\pi} \int_{-\pi}^{+\pi} d\phi \int_0^{\pi} d\theta \frac{1}{\sin^3\theta \cos^4\phi} \xi^2 \left[X_1(\mathbf{k}, s_x) + X_3(\mathbf{k}, s_x) \right] ,$$

$$\alpha_{yz}^*(\xi_*, \mathcal{G}_*) = \frac{1}{2\pi} \int_{-\pi}^{+\pi} d\phi \int_0^{\pi} d\theta \frac{1}{\sin^3\theta \cos^4\phi} \xi^2 \left[X_2(\mathbf{k}, s_x) + X_4(\mathbf{k}, s_x) \right] .$$

As previously, it is not possible to relate these quantities in a straightforward manner to the energy density (9) and the density of the gradient forcing (10) and the calculation will be carried out in the case of a weak inhomogeneity in Section VI. However, a few interesting observations can be made regarding the structure of the γ and α effects. First, Eq. (38) shows that the γ effect is bi-dimensional in the plane of the shear. Second, without shear ($\mathcal{A} = 0$), analysis of the two first equations of (40) shows that $\gamma_x^* \neq 0$ and $\gamma_y^* = 0$. This is in agreement with previous results[12]: when inhomogeneity is the only source of preferred direction, the α effect vanishes and the magnetic pumping is aligned with the inhomogeneity. On the other hand, the analysis of the α effect in Eq. (39) shows that there are only non diagonal components in the α tensor (α_{xz} and α_{yz}). Third, without shear ($\mathcal{A} = 0$), a closer analysis of the two last equations of (40) shows that $\alpha_{xz}^* \neq 0$ and $\alpha_{yz}^* = 0$. That is, there is no α effect without shear.

B.   Inhomogeneity in the z direction

By substituting Eq. (27) in Eq. (33), the tensor a_{ij} can be obtained in the following form:

$$a_{ij} = \frac{\tau_f}{(2\pi)^3 \mathcal{A}^2} \int d\mathbf{k} \int ds_z \, e^{is_z z} \, (ik_y) \frac{E(k, s_z)}{16\pi k^2} \begin{pmatrix} Z_1(\mathbf{k}, s_z) & Z_3(\mathbf{k}, s_z) & 0 \\ Z_2(\mathbf{k}, s_z) & Z_4(\mathbf{k}, s_z) & 0 \\ 0 & 0 & Z_5(\mathbf{k}, s_z) \end{pmatrix}_{ij} . \quad (41)$$

Components that would vanish upon $\mathbf{k}$-angular integration were not shown in Eq. (41). In Eq. (41), the following integrals are defined

$$Z_1(\mathbf{k}, s_z) = \int_a^{+\infty} d\tau e^{-2\xi\{Q(\tau)-Q(a)\}} \left[f_{11} \left(J_{y1}^- K_{z1}^+ - J_{z1}^- K_{y1}^+ \right) + f_{22} \left(J_{z2}^- K_{y2}^+ - J_{y2}^- K_{z2}^+ \right) \right. \quad (42)$$
$$\left. + f_{12} \left(J_{z1}^- K_{z1}^+ - J_{z2}^- K_{y1}^+ \right) - f_{21} \left(J_{z1}^- K_{y2}^+ + J_{y1}^- K_{z2}^+ \right) \right] ,$$

$$Z_2(\mathbf{k}, s_z) = \int_a^{+\infty} d\tau e^{-2\xi\{Q(\tau)-Q(a)\}} f_{11} \left(J_x^- K_{z1}^+ - J_{z1}^- K_x^+ + f_{12} J_{z2}^- K_x^+ - f_{21} J_x^- K_{z2}^+ \right) ,$$

$$Z_3(\mathbf{k}, s_z) = \int_a^{+\infty} d\tau e^{-2\xi\{Q(\tau)-Q(a)\}} \left[f_{11} \left(J_{y1}^- L_{z1}^+ - J_{z1}^- L_{y1}^+ \right) + f_{22} \left(J_{z2}^- L_{y2}^+ - J_{y2}^- L_{z2}^+ \right) \right.$$

$$+f_{12}\left(J_{21}^{-}L_{z1}^{+}-J_{z2}^{-}L_{y1}^{+}\right)-f_{21}\left(J_{z1}^{-}L_{y2}^{+}+J_{y1}^{-}L_{z2}^{+}\right)\Big]\ ,$$

$$Z_4(\mathbf{k},s_z)=\int_a^{+\infty}d\tau e^{-2\xi\{Q(\tau)-Q(a)\}}f_{11}\left(J_x^{-}L_{z1}^{+}-J_{z1}^{-}L_x^{+}+f_{12}J_{z2}^{-}L_x^{+}-f_{21}J_x^{-}L_{z2}^{+}\right)\ ,$$

$$Z_5(\mathbf{k},s_z)=(\beta+\mathcal{G})\int_a^{+\infty}e^{-2\xi\{Q(\tau)-Q(a)\}}f_{11}\left(J_{y1}^{-}L_x^{+}-J_x^{-}L_{y1}^{+}\right)\ .$$

Here, $\xi=\nu k_y^2/\mathcal{A}$, $Q(x)=\kappa x+x^3/3+\mathcal{G}^2x$, and $\mathcal{G}=s_z/(2k_y)$.

From the tensor a_{ij} in Eq. (41), the turbulent transport of magnetic flux and the α effect are obtained as:

$$\boldsymbol{\gamma}=\frac{\tau_f}{(2\pi)^3}\int d\mathbf{k}\int ds_z\,e^{is_zx}\frac{E(k,s_z)}{16\pi\nu^2k_y^4k^2}(ik_y)\,\xi^2\begin{pmatrix}0\\0\\Z_2(\mathbf{k},s_z)-Z_3(\mathbf{k},s_z)\end{pmatrix}\ ,\qquad(43)$$

and

$$\alpha_{ij}=\frac{\tau_f}{(2\pi)^3}\int d\mathbf{k}\int ds_z\,e^{is_zz}\frac{E(k,s_z)}{8\pi\nu^2k_y^4k^2}(ik_y)\,\xi^2\times\qquad(44)$$

$$\begin{pmatrix}2Z_1(\mathbf{k},s_z) & Z_2(\mathbf{k},s_z)+Z_3(\mathbf{k},s_z) & 0\\Z_2(\mathbf{k},s_z)+Z_3(\mathbf{k},s_z) & 2Z_4(\mathbf{k},s_z) & 0\\0 & 0 & 2Z_5(\mathbf{k},s_z)\end{pmatrix}_{ij}\ .$$

To find the overall behavior of the γ and α effects, all possible values of $\mathbf{k}$ have to be considered and the integration over $\mathbf{k}$ has to be performed as in the previous section. This k integration can be shown to reduce Eqs. (43) and (44) to

$$\boldsymbol{\gamma}=-\frac{\tau_f}{(2\pi)^2}\int_0^{+\infty}dk\int_{-\infty}^{+\infty}ds_z\,\sin[s_zz]\frac{E(k,s_z)}{8\pi\nu^2k^3}\begin{pmatrix}0\\0\\\gamma_z^*(\xi_*,\mathcal{G}_*)\end{pmatrix}\ ,\qquad(45)$$

and

$$\alpha_{ij}=-\frac{\tau_f}{(2\pi)^2}\int_0^{+\infty}dk\int_{-\infty}^{+\infty}ds_z\,\sin[s_zz]\frac{E(k,s_z)}{8\pi\nu^2k^3}\begin{pmatrix}\alpha_{xx}^*(\xi_*,\mathcal{G}_*) & \alpha_{xy}^*(\xi_*,\mathcal{G}_*) & 0\\\alpha_{xy}^*(\xi_*,\mathcal{G}_*) & \alpha_{yy}^*(\xi_*,\mathcal{G}_*) & 0\\0 & 0 & \alpha_{zz}^*(\xi_*,\mathcal{G}_*)\end{pmatrix}_{ij}\quad(46)$$

In Eqs (45-46), the following coefficients are functions only of $\xi_*=\nu k^2/\mathcal{A}$ and $\mathcal{G}_*=s_z/(2k)$:

$$\gamma_z^*(\xi_*,\mathcal{G}_*)=\frac{1}{2\pi}\int_{-\pi}^{+\pi}d\phi\int_0^{\pi}d\theta\frac{1}{\sin^3\theta\cos^4\phi}\xi^2\left[Z_2(\mathbf{k},s_z)-Z_3(\mathbf{k},s_z)\right]\ ,\qquad(47)$$

$$\alpha_{xx}^*(\xi_*,\mathcal{G}_*)=\frac{1}{2\pi}\int_{-\pi}^{+\pi}d\phi\int_0^{\pi}d\theta\frac{1}{\sin^3\theta\cos^4\phi}\xi^2Z_1(\mathbf{k},s_z)\ ,$$

16

$$\alpha_{yy}^*(\xi_*, \mathcal{G}_*) = \frac{1}{2\pi} \int_{-\pi}^{+\pi} d\phi \int_0^\pi d\theta \frac{1}{\sin^3 \theta \cos^4 \phi} \xi^2 Z_1(\mathbf{k}, s_z) \, ,$$

$$\alpha_{zz}^*(\xi_*, \mathcal{G}_*) = \frac{1}{2\pi} \int_{-\pi}^{+\pi} d\phi \int_0^\pi d\theta \frac{1}{\sin^3 \theta \cos^4 \phi} \xi^2 Z_5(\mathbf{k}, s_z) \, ,$$

$$\alpha_{xy}^*(\xi_*, \mathcal{G}_*) = \frac{1}{2\pi} \int_{-\pi}^{+\pi} d\phi \int_0^\pi d\theta \frac{1}{\sin^3 \theta \cos^4 \phi} \xi^2 [Z_2(\mathbf{k}, s_z) + Z_3(\mathbf{k}, s_z)] \, .$$

As previously, it is not possible to relate these quantities directly to the energy density (9) and the density of the gradient forcing (10) and the calculation will be carried out in the case of a weak inhomogeneity in Section VI. However, a few interesting observations can be made regarding the structure of the γ and α effects. First, Eq. (45) shows that the γ effect is unidimensional and perpendicular to the plane of the shear. Second, without shear ($\mathcal{A} = 0$), a closer analysis of the first equation of (47) shows that $\gamma_z^* \neq 0$. This is in agreement with previous results[12]: when inhomogeneity is the only source of preferred direction, the α effect vanishes and the magnetic pumping is aligned with the inhomogeneity. Third, with regard to the α effect, Eq. (46) shows that there are three diagonal components in the α tensor and one off-diagonal component (recall that α is a symmetric tensor, i.e. $\alpha_{xy} = \alpha_{yx}$). Finally, without shear ($\mathcal{A} = 0$), analysis of the last four equations of (40) shows that all the components of the α effect vanish without shear.

VI.   WEAK INHOMOGENEITY

As mentioned previously, to find the overall dependence of the magnetic pumping and α effects on the shear, one needs to perform the integration over the $\mathbf{s}$ variables, characterizing the scale of the inhomogeneity. This requires us to prescribe the dependence of the forcing on $\mathbf{s}$ and perform the integration for all values of $\mathbf{x}$. Since this is numerically too demanding, we compute exactly only in the case of a weak inhomogeneity. To this end, we first write the function defined in Eqs. (22), (24), (29), (40) and (47) in powers of the inhomogeneity parameter $\mathcal{G}_* \ll 1$:

$$I_i^*(\xi_*, \mathbf{s}) = I_i^0(\xi_*) + I_i^2(\xi_*)\mathcal{G}_*^2 + \dots \, , \tag{48}$$

$$H^*(\xi_*, \mathcal{G}_*) = H^1(\xi_*)\mathcal{G}_* + H^3(\xi_*)\mathcal{G}_*^3 + \dots \, ,$$

$$\gamma_i^*(\xi_*, \mathcal{G}_*) = \gamma^1(\xi_*)\mathcal{G}_* + \gamma^3(\xi_*)\mathcal{G}_*^3 + \dots \, ,$$

$$\alpha_{ij}^*(\xi_*, \mathcal{G}_*) = \alpha_{ij}^1(\xi_*)\mathcal{G}_* + \alpha_{ij}^3(\xi_*)\mathcal{G}_*^3 + \dots \, .$$

Keeping only the leading order terms by assuming that

$$\int_{-\infty}^{+\infty} s^2 \cos[\mathbf{s} \cdot \mathbf{x}] E(k, s) ds \ll \int_{-\infty}^{+\infty} \cos[\mathbf{s} \cdot \mathbf{x}] E(k, s) ds , \tag{49}$$

turbulent intensity and helicity are obtained in the following form:

$$\langle u_x^2 \rangle = \frac{\tau_f}{(2\pi)^2} \int_0^{+\infty} dk I_x^0(\xi_*) E_0(k, \mathbf{s}) , \tag{50}$$

$$\langle u_y^2 \rangle = \frac{\tau_f}{(2\pi)^2} \int_0^{+\infty} dk I_y^0(\xi_*) E_0(k, \mathbf{s}) ,$$

$$\langle u_z^2 \rangle = \frac{\tau_f}{(2\pi)^2} \int_0^{+\infty} dk I_z^0(\xi_*) E_0(k, \mathbf{s}) ,$$

$$\langle \mathbf{u} \cdot \nabla \times \mathbf{u} \rangle = -\frac{\tau_f}{(2\pi)^2} \int_0^{+\infty} dk H^1(\xi_*) G_0(k, \mathbf{s}) .$$

Here $E_0(k, \mathbf{s})$ and $G_0(k, \mathbf{s})$ are the spectra for the kinetic energy and the inhomogeneity gradient which have been defined in Eqs. (9) and (10). The turbulence intensity is shown on Figure 1 for inhomogeneity in the x and z directions; the helicity is shown on Figure 2 for inhomogeneity in the z direction (the helicity vanishes for inhomogeneity in the x direction). In either case when the shear is in the x or z-direction, a weak shear increases the turbulent intensity. It is because a large-scale shear flow transfers energy toward small-scale thus strengthening small-scale turbulence. On the other hand, for strong shear, the turbulent intensity is decreasing with shear, ultimately vanishing for sufficiently strong shear. This is due to shear stabilization which damps turbulence and reduces transport: flow shear facilitates the cascade of various quantities such as energy to small scales, enhancing the dissipation rate[15] and thus leading to weak turbulence. A similar behavior is observed for the turbulent helicity except for the fact that it is zero for vanishing shear whereas the turbulent intensity is small but non-zero in that case. That is, a shear flow, interestingly, causes non-zero flow helicity in inhomogeneous turbulence driven by a non-helical forcing.

As seen in the previous sections, not all the components of the γ and α effects are present. In the case where the inhomogeneity is in the x-direction, the magnetic pumping and α effect can be written as:

$$\boldsymbol{\gamma} = -\frac{\tau_f}{(2\pi)^2} \int_0^{+\infty} dk G_0(k) \begin{pmatrix} \gamma_x^1(\xi_*) \\ \gamma_y^1(\xi_*) \\ 0 \end{pmatrix} , \tag{51}$$
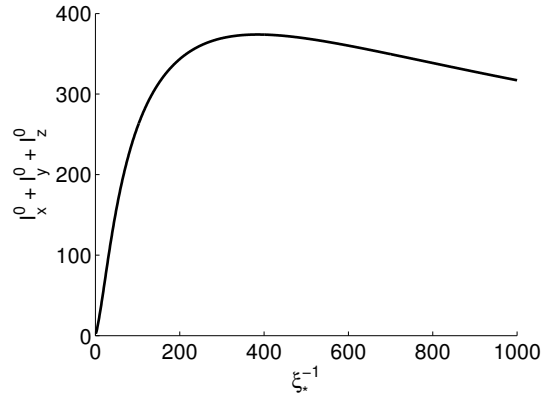
FIG. 1. Dependence of the function $I_x^0 + I_y^0 + I_z^0$ on the dimensionless shear $\xi_*^{-1} = \mathcal{A}/(\nu k^2)$. Note that the turbulence intensity is the same when the inhomogeneity is in the x and z direction.
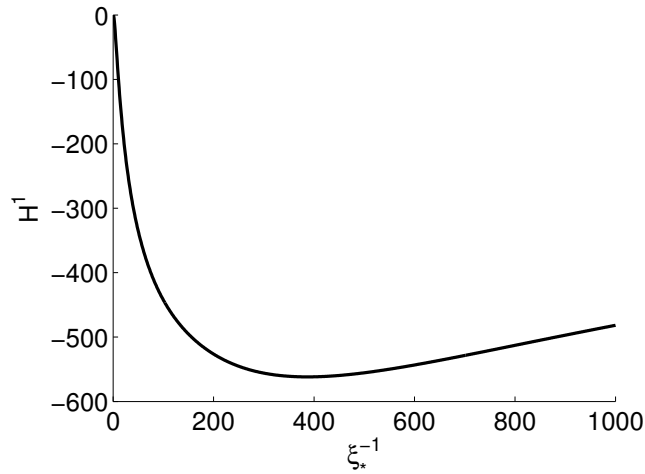

FIG. 2. Dependence of the function H^1 on the dimensionless shear $\xi_*^{-1} = \mathcal{A}/(\nu k^2)$ for inhomogeneity in the z-direction and for a weak inhomogeneity.

and

$$
\alpha_{ij} = -\frac{\tau_f}{(2\pi)^2} \int_0^{+\infty} dk G_0(k) \begin{pmatrix} 0 & 0 & \alpha_{xz}^1(\xi_*, \mathcal{G}_*) \\ 0 & 0 & \alpha_{yz}^1(\xi_*, \mathcal{G}_*) \\ \alpha_{xz}^1(\xi_*, \mathcal{G}_*) & \alpha_{yz}^1(\xi_*, \mathcal{G}_*) & 0 \end{pmatrix}_{ij} . \tag{52}
$$

Figures 3 shows the dependence of γ_x^1, γ_y^1, α_{xz}^1, and α_{yz}^1 on the dimensionless shear $\xi_*^{-1} = \mathcal{A}/(\nu k^2)$. Note that for $\xi_*^{-1} = 0$, we have $\gamma_x^1 \neq 0$, $\gamma_y^1 = 0$ and $\alpha_{xz}^1 = \alpha_{yz}^1 = 0$.

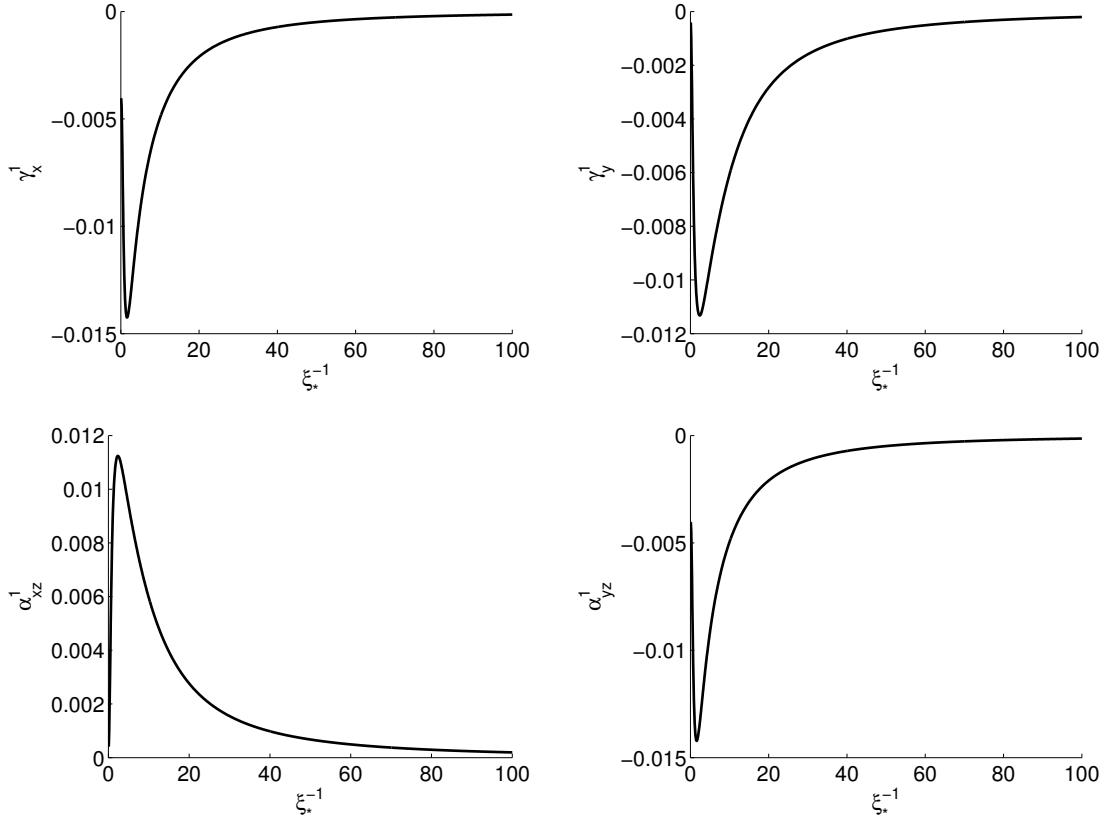In the case where the inhomogeneity is in the z-direction, the magnetic pumping and α

19

FIG. 3. Dependence of the coefficient γ_x^1, γ_y^1, α_{xz}^1, and α_{yz}^1 on the dimensionless shear $\xi_*^{-1} = \mathcal{A}/(\nu k^2)$. The inhomogeneity is in the plane of the shear (i.e. in the x-direction). Note that for $\xi_*^{-1} = 0$, we have $\gamma_x^1 \neq 0$, $\gamma_y^1 = 0$ and $\alpha_{xz}^1 = \alpha_{yz}^1 = 0$.

effect can be written as:

$$\boldsymbol{\gamma} = -\frac{\tau_f}{(2\pi)^2} \int_0^{+\infty} dk G_0(k) \begin{pmatrix} 0 \\ 0 \\ \gamma_z^1(\xi_*) \end{pmatrix}, \tag{53}$$

and

$$\alpha_{ij} = -\frac{\tau_f}{(2\pi)^2} \int_0^{+\infty} dk G_0(k) \begin{pmatrix} \alpha_{xx}^1(\xi_*) & \alpha_{xy}^1(\xi_*) & 0 \\ \alpha_{xy}^1(\xi_*) & \alpha_{yy}^1(\xi_*) & 0 \\ 0 & 0 & \alpha_{zz}^1(\xi_*) \end{pmatrix}_{ij}. \tag{54}$$

Figures 4 shows the dependence of the coefficient γ_z^1, α_{xx}^1, α_{yy}^1, α_{zz}^1, and α_{xy}^1 on the dimensionless shear $\xi_*^{-1} = \mathcal{A}/(\nu k^2)$. Note that For $\xi_*^{-1} = 0$, we have $\gamma_z^1 \neq 0$ and $\alpha_{xx}^1 = \alpha_{yy}^1 = \alpha_{zz}^1 = \alpha_{xy}^1 = 0$. The results in Figures 3 and 4 can be summarized as follows:
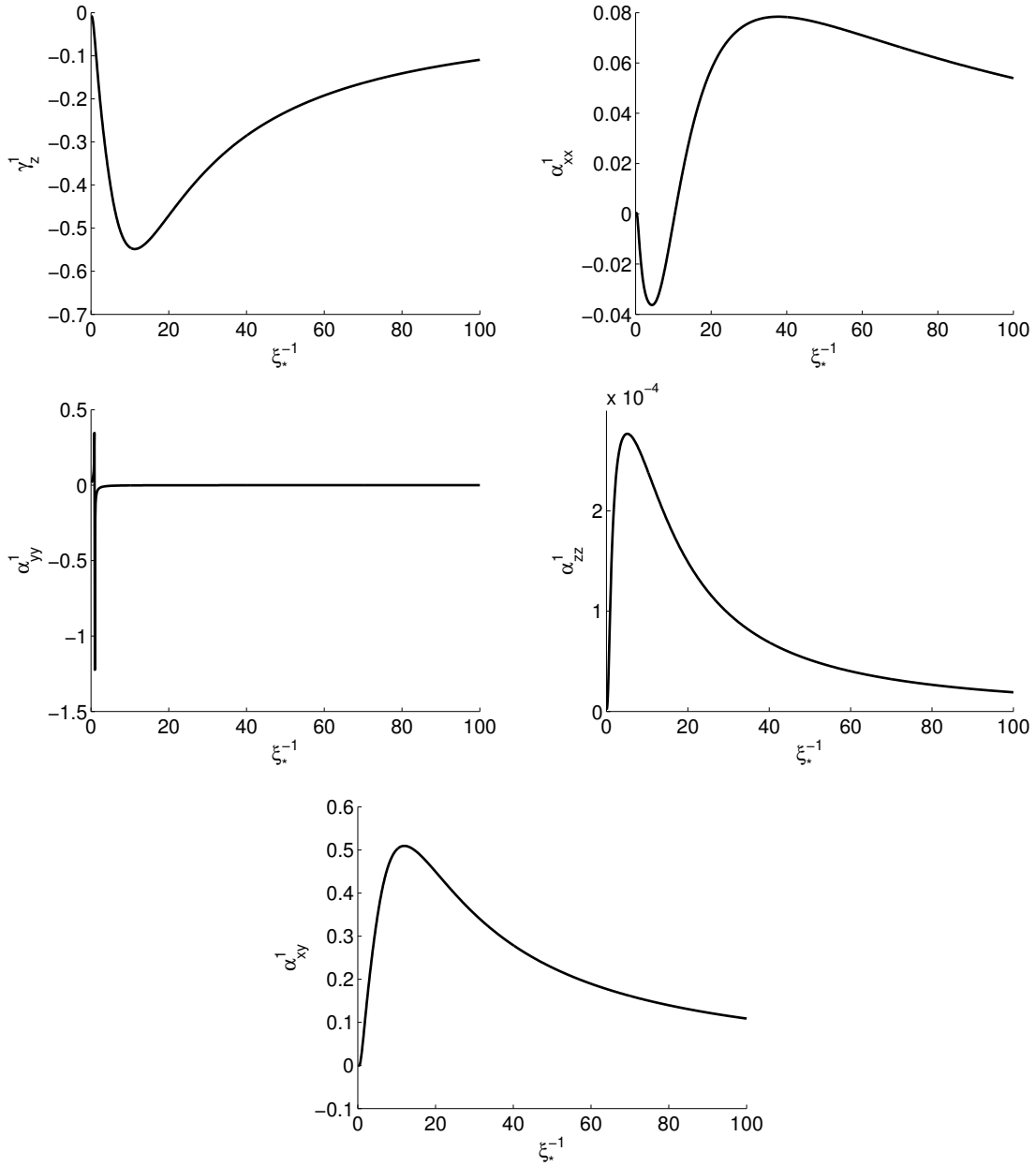
20

FIG. 4. Dependence of the coefficient γ_z^1, α_{xx}^1, α_{yy}^1, α_{zz}^1, and α_{xy}^1 on the dimensionless shear $\xi_*^{-1} = \mathcal{A}/(\nu k^2)$. The inhomogeneity is orthogonal to the plane of the shear (i.e. in the z-direction). Note that For $\xi_*^{-1} = 0$, we have $\gamma_z^1 \neq 0$ and $\alpha_{xx}^1 = \alpha_{yy}^1 = \alpha_{zz}^1 = \alpha_{xy}^1 = 0$.

- Without shear ($\mathcal{A} = 0$), the magnetic pumping is in the direction of the inhomogeneity and the α effect vanishes.

- For weak but non-vanishing shear, the magnetic pumping becomes bi-dimensional when the inhomogeneity is in the plane of the shear flow whereas it remains in the
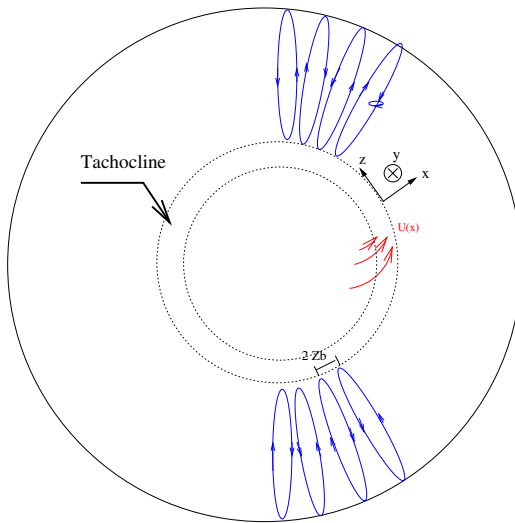
21

FIG. 5. Sketch of the mean-field dynamo model considered in this paper. Note that the dynamo equations are solved only in a thin layer where the shear is located (the tachocline) and that the convection in the outer-envelope provides the inhomogeneous forcing. Zb is the scale on which the forcing is varying (i.e. the size of a convective roll).

    direction of the inhomogeneity if the direction of the inhomogeneity is orthogonal to the plane of the shear flow.

- For weak but non-vanishing shear, the α effect increases with shear. Furthermore, when the inhomogeneity is in the plane of the shear, the α effect has only non-diagonal components. In contrast, when the inhomogeneity is orthogonal to the plane of the shear, the α effect has both diagonal and non-diagonal components.

- For sufficiently strong shear, both the γ and α effects vanish due to shear stabilization.

VII. A SIMPLE MEAN-FIELD DYNAMO MODEL

The previous sections show that α and γ effects can arise from the combined effect of a large-scale shear flow and an inhomogeneous forcing even in the absence of rotation. To demonstrate the possible existence of dynamo due to these two effects, we consider a simple mean-field dynamo model in which a large-scale magnetic field is amplified. This is a toy model of α-Ω dynamo in stars and is illustrated on Figure 5. Specifically, both the shear and the turbulence are assumed to be located inside a thin layer (the solar tachocline in the

22

case of the Sun) in the interior of the star. We use a (local) Cartesian coordinates where (x, y, z) are the radial, azimuthal and latitudinal coordinates. Note that for the Sun, the x-direction would correspond to the radial direction, e.g. in the tachocline it corresponds to the direction of the shear due to radial differential rotation. Consequently, the shear flow due to differential rotation is written $\langle \mathbf{U} \rangle = -\mathcal{A}x\mathbf{y}$. The turbulence in this layer is assumed to be triggered by an inhomogeneous forcing whose statistics is given by Eq. (6). From the physical point of view, this external forcing could be due to turbulent plumes coming from convection of the outer convective envelope. In that case, the forcing is likely to be highly inhomogeneous as the forcing ought to be stronger in places where the convective motions are parallel to the radial direction (see Figure 5). We express the magnetic field as the sum of a toroidal part $(\bar{B}(x, z)\mathbf{e}_y)$ and a poloidal part $[\nabla \times (\bar{A}(x, z)\mathbf{e}_y)]$. Note that $\mathbf{B}$ depends only on the (local) radial x and latitudinal z directions and is independent of the azimuthal coordinate y (i.e. it represents an axisymmetric field). The toroidal and poloidal components of this axisymmetric field are governed by the system of equation:

$$\partial_t \bar{B} = \mathcal{A}\partial_z \bar{A} + \partial_z \mathcal{E}_x - \partial_x \mathcal{E}_z + (\eta + \beta)\Delta \bar{B} , \qquad (55)$$

$$\partial_t \bar{A} = \mathcal{E}_y + (\eta + \beta)\Delta \bar{A} .$$

Here, the term proportional to β in Eq. (55) is the turbulent magnetic diffusivity which was computed in the kinematic limit in a previous contribution[21]:

$$\beta = \frac{\tau_f}{(2\pi)^2} \int_0^{+\infty} \frac{E(k, s_x)}{8\pi\nu^2 k^4} \beta^*(\xi_*) . \qquad (56)$$

Note that the effect of the inhomogeneity on the β effect[22] should be included in Eq. (56). However, this effect is expected to be very small in the weak inhomogeneity limit and thus Eq. (56) is used as an approximation for the turbulent diffusivity. The dependence of the coefficient β^* with shear is plotted on Figure 6.

Eq. (55) shows that there can be magnetic field amplification only if the component $\mathcal{E}_y$ does not vanish and depends on the toroidal component of the magnetic field $\bar{B}$. This implies that the diagonal component α_{yy} must be non-zero. As can be seen from Eqs. (39) and (46), this is the case only for an inhomogeneity in the z direction. Therefore, we study the case where the inhomogeneity is in the z direction and accordingly simplify Eq. (55) as:

$$\partial_t \bar{B} = \xi_*^{-1}\partial_z \bar{A} - \partial_z \left[b(\xi_*, z)\partial_z \bar{A} \right] - \partial_x \left[c(\xi_*, z)\partial_x \bar{A} \right] + \partial_z \left[a(\xi_*, z)\bar{B} \right] + \partial_z \left[d(\xi_*, z)\partial_z \bar{B} \right] + \partial_x \left[d(\xi_*, z)\partial_x \bar{B} \right] \quad (57)$$

$$\partial_t \bar{A} = -e(\xi_*, z)\partial_z \bar{A} + f(\xi_*, z)\bar{B} + d(\xi_*, z)\partial_{z^2} \bar{A} + d(\xi_*, z)\partial_{x^2} \bar{A} .$$
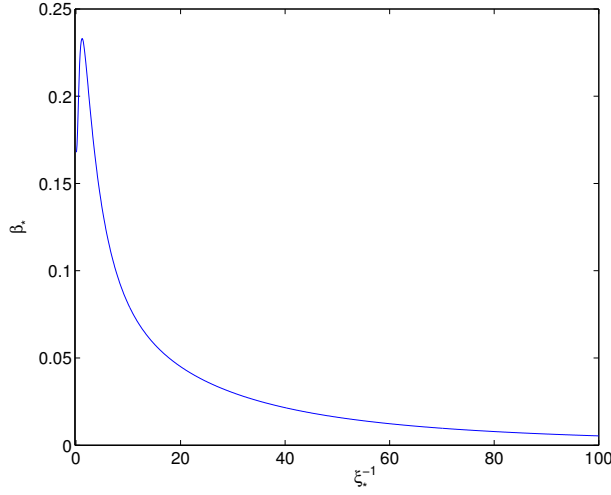
FIG. 6. Dependence of the coefficient β^* on the dimensionless shear $\xi_*^{-1} = \mathcal{A}/(\nu k^2)$,

.

Here, the units are non-dimensionalized by using the turbulent length scale l and the diffusion time l^2/η; the coefficients are defined as:

$$a(\xi_*, z) = -\frac{\nabla\langle f^2\rangle}{64\eta^4 k^7}\left[\alpha_{xy}^* - \gamma_z^*\right] ,\qquad(58)$$

$$b(\xi_*, z) = -\frac{\nabla\langle f^2\rangle}{64\eta^4 k^7}\alpha_{xx}^* ,$$

$$c(\xi_*, z) = -\frac{\nabla\langle f^2\rangle}{64\eta^4 k^7}\alpha_{zz}^* ,$$

$$d(\xi_*, z) = \frac{\langle f^2\rangle}{32\eta^4 k^6}\beta^* ,$$

$$e(\xi_*, z) = -\frac{\nabla\langle f^2\rangle}{64\eta^4 k^7}\left[\alpha_{xy}^* + \gamma_z^*\right] ,$$

$$f(\xi_*, z) = -\frac{\nabla\langle f^2\rangle}{64\eta^4 k^7}\alpha_{yy}^* .$$

The z-dependence of these functions comes from the fact that the forcing and its gradient depend on spatial coordinate $\mathbf{x}$. In the following, the dependence is prescribed to be:

$$\langle f^2\rangle = \frac{F_0}{N(z_0)}\frac{z_0^2}{z_0^2 + z^2} ,\qquad \text{i.e.}\qquad -\frac{\nabla\langle f^2\rangle}{2} = \frac{F_0}{N(z_0)}\frac{z_0^2 z}{(z_0^2 + z^2)^2} .\qquad(59)$$

Note that z_0 represents the length-scale on which the forcing is varying. We introduce the following normalization factor $N(z_0) = z_0/Z_b \arctan(Z_b/z_0)$ to enforce that the total forcing (averaged over the simulation box $[-Z_b\ Z_b]$) is independent of z_0 and equal to F_0. The

24

coefficients in Eq. (57) can then be rewritten as:

$$a(\xi_*, z) = -\tilde{F}_0 \frac{z_0^2 z}{(z_0^2 + z^2)^2} \left[\alpha_{xy}^* - \gamma_z^*\right] , \tag{60}$$

$$b(\xi_*, z) = -\tilde{F}_0 \frac{z_0^2 z}{(z_0^2 + z^2)^2} \alpha_{xx}^* ,$$

$$c(\xi_*, z) = -\tilde{F}_0 \frac{z_0^2 z}{(z_0^2 + z^2)^2} \alpha_{zz}^* ,$$

$$d(\xi_*, z) = \tilde{F}_0 \frac{z_0^2}{z_0^2 + z^2} \beta^* ,$$

$$e(\xi_*, z) = -\tilde{F}_0 \frac{z_0^2 z}{(z_0^2 + z^2)^2} \left[\alpha_{xy}^* + \gamma_z^*\right] ,$$

$$f(\xi_*, z) = -\tilde{F}_0 \frac{z_0^2 z}{(z_0^2 + z^2)^2} \alpha_{yy}^* ,$$

where $\tilde{F}_0 = F_0/(32\eta^4 k^6)$. Note that the ratio of the turbulent (β_*) and the molecular diffusivity (η) is of order $\tilde{F}_0$. The ratio of the two is the magnetic Reynolds number: $R_m \sim \tilde{F}_0$.

Eq. (57) is a partial differential equation (PDE) for two spatial and one time coordinates. By following Parker[23], we assume the typical variation in the radial direction (x) to be of order μ^{-1} and approximate the spatial derivative with respect to x as $\partial_x^2 F \sim -\mu^2 F$. In the following, the value $\mu^{-1} = 0.05 R_o/l$ is used corresponding to a shearing region (the tachocline in the solar case) of extent 5% of the solar radius R_o (note that all quantities are non-dimensionalized by the turbulent length scale l). With these assumptions, Eq. (57) reduces to the following 1D-PDE system of equations:

$$\partial_t \bar{B} = \xi_*^{-1} \partial_z \bar{A} - \partial_z \left[b(\xi_*, z)\partial_z \bar{A}\right] + \mu^2 c(\xi_*, z)\bar{A} + \partial_z \left[a(\xi_*, z)\bar{B}\right] + \partial_z \left[d(\xi_*, z)\partial_z \bar{B}\right] - \mu^2 d(\xi_*, z)\bar{B} \tag{61}$$

$$\partial_t \bar{A} = -e\partial_z \bar{A} + f\bar{B} + d(\xi_*, z)\partial_{z^2} \bar{A} - \mu^2 d(\xi_*, z)\bar{A} .$$

The parameters are fixed by characteristic value of the tachocline: $\tilde{F}_0 \sim R_m = 10^5$ (e.g. see Ref.[24]). The following equality between the turbulent length scale and the solar radius (R_o) is assumed: $l \sim R_m^{-1} R_o$. This suggests the value of the parameter μ to be roughly $\mu = 0.0002$. Other parameters to be fixed are the size of the box of the simulation $2Z_b$ (z varying from $-Z_b$ to $+Z_b$) and the boundary conditions. First, as can be seen from Figure 5, the scale of the inhomogeneity is set by the size of a convective cell. The size of the box is thus chosen to be $2Z_b = 10000$ corresponding to 10 convective cells per hemisphere. Second the boundary condition is fixed to be a vanishing magnetic field at the boundaries:
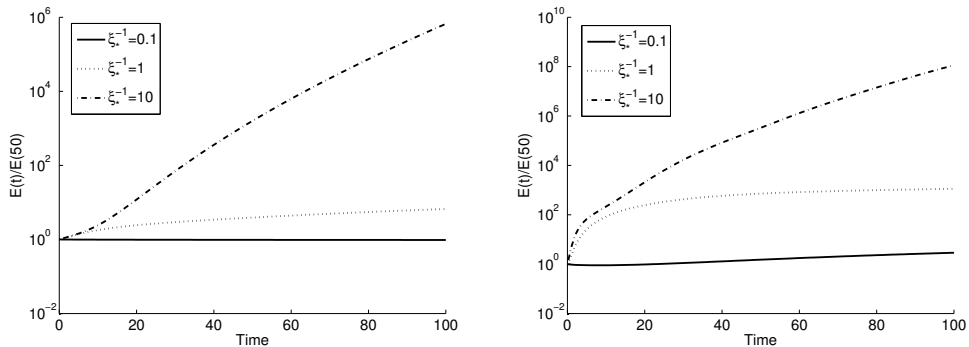
FIG. 7. Evolution of the magnetic energy with time for different values of the dimensionless shear $\xi_*^{-1} = \mathcal{A}/(\nu k^2)$. The left-hand panel is for $z_0 = 10$ and the right-hand panel is for $z_0 = 1000$. The other parameters are fixed to $\mu = 0.0002$ and $\tilde{F}_0 = 10^5$.

$\bar{A}(t,z) = \bar{B}(t,z) = 0$ for $z = \pm Z_b$ and system (61) is solved using MATLAB PDE solver. Note that periodic boundary conditions can also be used as more than one convective cell forcing the turbulence is expected in the tachocline. For simplicity and in order to identify key aspects in the generation of magnetic field, we only consider fixed boundary conditions in this paper. Figure 7 shows the magnetic energy defined as $E(t) = \int dz[A(z,t)^2 + B(z,t)^2]$ for different values of the shear parameter ξ_*^{-1} and for two values of z_0. Note that the larger value of z_0 represents a wider distribution of inhomogeneity. It is seen that there is dynamo for $z_0 = 10$ and $z_0 = 1000$ provided that the shear is strong enough. In order to investigate the spatial structure of the growing magnetic field, we show in Figure 8 a spatio-temporal diagram of the magnetic field in the case $z_0 = 1000$ and $\xi_*^{-1} = 10$. The x and y axes show the time and the z-direction, respectively; the color coding represents the intensity of the toroidal magnetic field (on the left) and the poloidal magnetic field (on the right). This shows that the magnetic field is created near $z = 0$ and that it is migrating towards the boundary of the domain as time goes by. To understand this, recall that the β-effect (the turbulent diffusion) is strongest at $z = 0$. In comparison, a simple calculation shows that the gradient of the forcing, and consequently the γ and α effect, is maximum at $z = \pm z_0/\sqrt{3}$. This is illustrated on Figure 9 which shows the profile of the forcing intensity and its gradient. Since $\gamma_z^1 < 0$ (see Figure 4), the pumping effect expels the magnetic field from $z = 0$ towards the boundary of the domain. These profiles of α and γ thus imply that the magnetic field is created near $z = \pm z_0/\sqrt{3}$ and is expelled towards the boundaries of
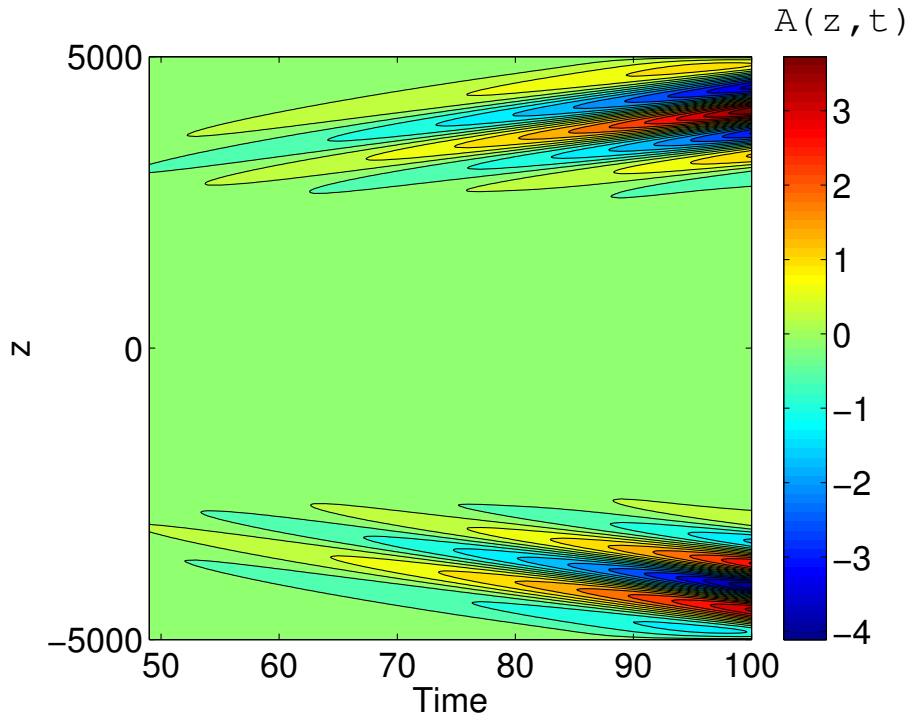
26

FIG. 8. Spatio-temporal diagram of the growing magnetic field. The parameters are fixed to $\mu = 0.0002$, $\tilde{F}_0 = 10^5$, $z_0 = 1000$ and $\xi_*^{-1} = 10$.

the domain.

Figure 10 shows the spatial structure of the magnetic field at late times ($t = 100$). It is easy to see that the magnetic field is concentrated near the boundaries of the integration domain. Furthermore, one can see that the magnetic field is oscillating near the boundary. This is to be expected as the magnetic energy has to accumulate on the boundary of the domain while preserving the boundary condition $\bar{A}(\pm Z_b, t) = \bar{B}(\pm Z_b, t) = 0$. Note that for periodic boundary conditions, there might not be such an oscillation as the magnetic field could take any value on the border of the domain.

To summarize, a simple mean field dynamo model with differential rotation and inhomogeneous γ and α effects is introduced. The magnetic field is shown to be created primarily where the gradient of the forcing is the strongest. Due to magnetic pumping (γ effect), the magnetic field is expelled from the region of the strongest inhomogeneity and migrates towards the region where the inhomogeneity is the weakest. We also observe that the magnetic field is oscillating more and more as time goes by. Due to the simplicity of our mean-field model (e.g. boundary conditions), some of these results might be unphysical. Specifically, we
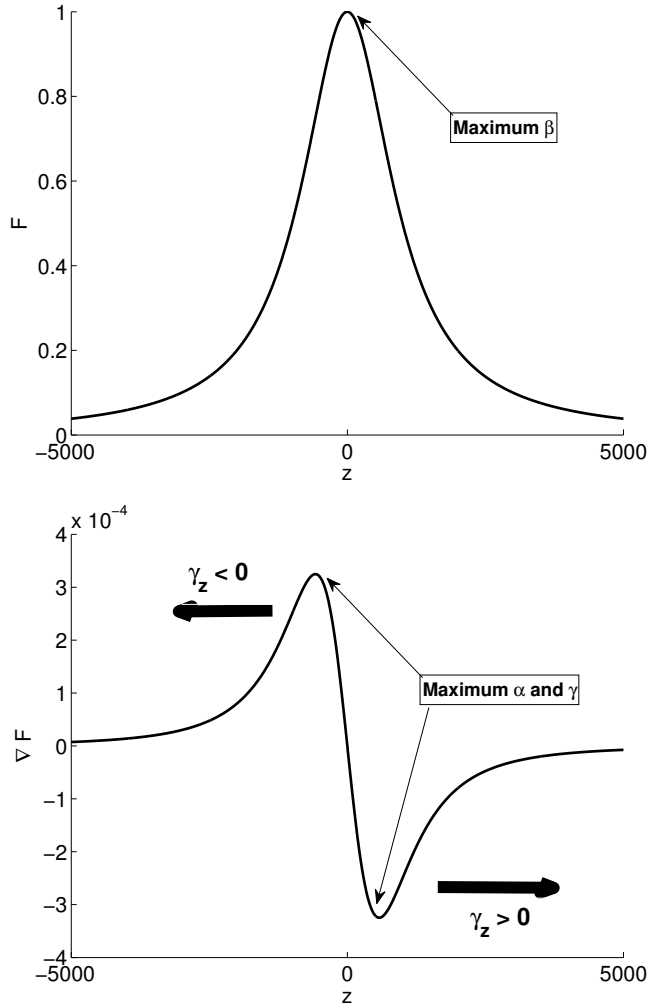
27

FIG. 9. Sketch of the spatial structure of the intensity of the forcing (left) and its gradient (right) for a parameter $z_0 = 1000$. On the right we put the sign of the magnetic pumping in the z direction: $\gamma_z = \gamma_z^1 \nabla F$ with $\gamma_z^1 < 0$.

expect the magnetic field generation and the migration of the magnetic field to the boundaries as suggested by the sketches in Figure 9. However, the oscillations of the magnetic field near boundaries may be artifact due to the boundary conditions of vanishing magnetic fields.

VIII.   CONCLUSION

This paper provided a theoretical prediction of the electromotive force induced in a sheared turbulence driven by a non-helical inhomogeneous forcing. Without shear, the
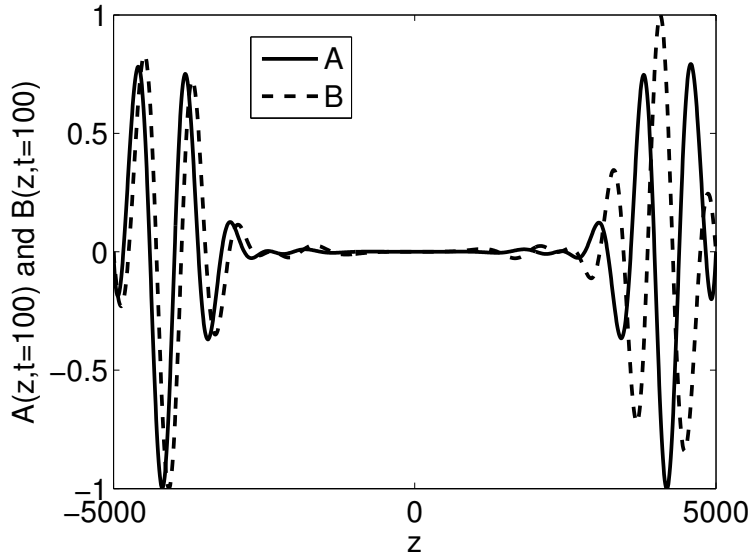
FIG. 10. Spatial structure of the magnetic field. The parameters are fixed to $\mu = 0.2$, $\tilde{F}_0 = 100$, $z_0 = 0.1$ and $\xi_*^{-1} = 10$.

electromotive force reduces to a magnetic pumping γ parallel to the direction of the inhomogeneity. As shear is increased, an additional component of the γ effect appears in the perpendicular (y) direction when the inhomogeneity is in the x-direction. Furthermore, the α effect, which vanishes without shear as expected, was shown to arise due to the combined effects of the inhomogeneous forcing and the shear. The structure of this α effect depends on the direction of the inhomogeneity. Specifically, when the inhomogeneity is in the direction of the shear (x), the α effect has only two non-zero off-diagonal components whereas in the case of an inhomogeneity in the z direction, perpendicular to shear flow, the α effect involves all three diagonal components and one off-diagonal component. For sufficiently strong shear, both α and γ effects are however reduced by shear stabilization: a strong shear favors a cascade of energy towards small scales and therefore increases the dissipation in the system[15], leading to weak turbulent transport. We note that this shear induced kinematic dynamo in inhomogeneous turbulence can intuitively be understood from symmetry considerations.

By using the theoretical prediction, the possibility of an axisymmetric (y-independent) mean-field dynamo due to the combined effect of an inhomogeneous forcing and a large-scale shear flow is investigated. By numerically solving a simplified model of alpha-Omega dynamo, we show that a coherent magnetic field is created primarily where the gradient of

the forcing is the strongest. Due to magnetic pumping (gamma effect), the magnetic field is then expelled from the region of the strongest inhomogeneity and migrates towards the region where the inhomogeneity is the weakest. The growing magnetic field thus tends to accumulate in the region of weakest forcing intensity.

This could have interesting implications for the structure of magnetic field in non-rotating stars. Since various sources of inhomogeneity are present due to convection in the outer envelope (see Figure 5), our results suggest that a strong magnetic field is likely to be observed in the middle of every convection cell where the inhomogeneity is weakest. In this case, a strong magnetic field would be observed at various latitude corresponding to the location of convective cells, leading to a series of stripes on the surface of the star. Furthermore, this pattern is likely to be stationary. It is interesting to contrast this to what is observed on the Sun where the dynamo is a result of differential rotation and alpha effect with opposite signs in the two hemispheres. In that case, sunspots (corresponding to a strong magnetic field) appear around a mid-latitude and migrates towards the equator, leading to the well-known butterfly diagram.

Finally, it is worth emphasizing that the purpose of this paper was to elucidate some key aspects of dynamos in sheared, inhomogeneous turbulence without a (global) rotation. The understanding of coherent magnetic fields in astrophysical and laboratory plasmas in general would involve other physical processes that were not included in this paper, i.e., $\mathbf{\Omega} \times \mathbf{J}$ effect[25], $\mathbf{W} \times \mathbf{J}$ effect[14], magnetic instabilities[26], etc, as well as the extension to nonlinear dynamos by including backreaction of magnetic fields. This will be investigated in future papers.

REFERENCES

[1] F. Cattaneo and D. W. Hughes, Mon. Not. R. Astron. Soc., **395**, L48 (2009)

[2] D. W. Hughes and M. R. E. Proctor, Phys. Rev. Lett., **102**, 044501 (2009)

[3] P. J. Käpylä, M. J. Korpi, and A. Brandenburg, Astron. Astrophys., **491**, 353 (2008)

[4]P. J. Käpylä, M. J. Korpi, and A. Brandenburg, Astron. Astrophys., **500**, 633 (2009)

[5]T. A. Yousef, T. Heinemann, A. A. Schekochihin, N. Kleeorin, I. Rogachevskii, A. B. Iskakov, S. C. Cowley, and J. C. McWilliams, Phys. Rev. Lett., **100**, 184501 (2008)

[6]M. R. E. Proctor, Mon. Not. R. Astron. Soc., **382**, L39 (2007)

[7]E. G. Blackman, Astrophys. J., **496**, L17 (1998)

[8]E. T. Vishniac and J. Cho, Astrophys. J, **550**, 752̆2013 (2001)

[9]V. Urpin, Phys. Rev. E, **65**, 026301 (2002)

[10]H. K. Moffatt, *Magnetic field generation in fluids* (CUP, 1978)

[11]F. Krause and K.-H. Rädler, *Mean field MHD and dynamo theory* (Pergamon press, 1980)

[12]K.-H. Rädler and R. Stepanov, Phys. Rev. E, **73**, 056311 (2006)

[13]L. L. Kichatinov and G. Rüdiger, Astron. Astrophys., **260**, 494 (1992)

[14]I. Rogachevskii and N. Kleeorin, Phys. Rev. E, **68**, 036301 (2003)

[15]K. H. Burrell, Phys. Plasmas, **4**, 1499 (1997)

[16]A. M. Savill, Ann. Rev. Fluid Mech., **19**, 531 (1987)

[17]N. Leprovost and E. Kim, Geophys. Astrophys. Fluid Dyn., **104**, 167 (2010)

[18]L. L. Kichatinov, Geophys. Astrophys. Fluid Dyn., **38**, 273 (1987)

[19]W. Kelvin, Philos. Mag., **24**, 188 (1887)

[20]E. Kim, Astron. Astrophys., **441**, 763 (2005)

[21]N. Leprovost and E. Kim, Astrophys. J., **696**, L125 (2009)

[22]P. H. Roberts and A. M. Soward, Astron. Nachr., **296**, 49 (1975)

[23]E. N. Parker, Astrophys. J., **122**, 293 (1955)

[24]S. M. Tobias, P. H. Diamond, and D. W. Hughes, Astrophys. J, **667**, L113 (2007)

[25]K.-H. Rädler, N. Kleeorin, and I. Rogachevski, Geophys Astrophys. Fluid Dyn., **67**, 249 (2003)

[26]M. S. Miesch, Astrophys. J, **658**, L131 (2007)